WAVE INDUCED VELOCITIES CLOSE TO A RIPPLED BED

by

C.G. du Toit*

The results are reported of velocity measurements in oscillatory flow over rippled beds. Velocities were measured with a laser-doppler anemometer in both an oscillating tray rig and an oscillatory flow U-tube. Both self-formed and artificial ripples were examined.

The results obtained in the two test rigs were compared and it was concluded that the flow fields obtained in the two cases were dynamically similar.

Measurements of the flow field clearly showed the formation, growth and ejection of vortices, as well as a strong surge of fluid over the ripples during and after flow reversal.

1 INTRODUCTION

A proper knowledge of the flow field in the boundary layer above the ripples on the sea bed is of considerable importance to the coastal engineer. It is essential to be able to fully understand the phenomena of sediment transport and energy dissipation.

A great deal of theoretical work has already been done on the subject and three different approaches can be distinguished. Firstly, it is assumed that the concepts used for turbulent boundary layers in steady flow over rough beds may be extended to oscillatory flow and that the vertical velocities may be neglected. Secondly, it is assumed that the mean velocity distribution may be well represented by a laminar solution if the exchange of momentum from one fluid layer to another is dominated by the mixing produced by the vortices rather than by the much smaller-scale turbulent eddies. Thirdly, a solution has been put forward, based on the "discrete vortex" method.

A number of experimental studies have also been made of the velocity distribution close to beds in oscillatory flow. However, in most cases the beds were essentially flat or the bed profiles did not closely resemble those of naturally occuring ripples. Horikawa & Watanabe (1970) and Nakato et al (1977) did measure velocities above natural sand ripples in oscillatory flow. They were, however, primarily interested in the turbulence

*Senior Lecturer, Department of Civil Engineering, University of Stellenbosch, Stellenbosch 7600, South Africa.

and suspended sediment distribution. A more detailed study of the flow field was made by Sawamoto et al (1980). They measured the velocities above a fixed ripple in an oscillatory flow wind tunnel.

The objective of this paper is to give a short account of measurements that were made of the flow fields above both artificial and natural sand ripples. A comparison of the various available theories with the data has already been made elsewhere by Du Toit & Sleath (1981).

2. EXPERIMENTAL EQUIPMENT

Experiments were carried out both in an oscillating tray rig and an oscillatory flow U-tube.

The oscillating tray rig is shown in Figure 1.
It consisted essentially of a flat tray 0.305 m wide which was oscillated in its own plane in a tank of still water. Simple harmonic motion was created by means of a variable speed motor with feed-back control driving a Scotch Yoke. Baffles, extending down to close to the bed, divided the tank into three sections. These baffles were to prevent vortices shed by the end of the tray from propagating into the central test section. Flow under these baffles were inhibited by compensating cylinders which had the same cross-sectional area as the tray.

Figure 2 shows a sketch of the oscillatory flow U-tube.
It consisted of a U-tube in which the water was caused to oscillate by a paddle driven, via a crank arm, by a variable speed motor with feed-back control. The central test section was 0.305 m wide and 0.45 m high. The arm containing the paddle was circular in section with an area 3.3 times that of the rest of the tube.

The oscillating tray rig could be operated over a wide range of strokes and periods of oscillation, whereas the oscillatory flow U-tube was restricted to periods close to its resonant period of 4.6 s.

The velocities were measured with a laser-doppler anemometer system. With the equipment available it was only possible to measure one component of velocity. The results given below are all for the horizontal component of velocity.

Phases were measured with the aid of a beam of light falling on a photo-electric cell for the oscillating tray rig. A flat plate, rigidly attached to the Scotch Yoke, interrupted the beam of light as the tray passed through the top dead-centre position. For the oscillatory flow U-tube the output from a resistance gauge in the open arm of the tube was used as a phase marker.

The outputs from the laser-doppler system and the phase marker were recorded on magnetic tape and subsequently fed through an analog-to-digital converter into a computor for analysis.

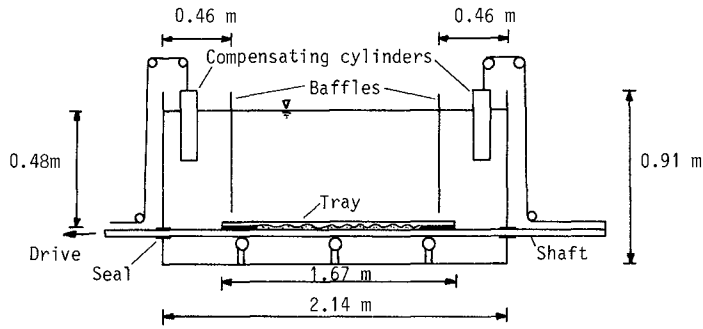

FIG. 1 Sketch of oscillating tray tank

Analog-to-digital conversion was carried out at a rate of between 600 and 720 samples per cycle.

All the tests with natural sand ripples were carried out with a sand of median diameter 0.41 mm, standard deviation 0.10 mm and specific gravity 2.65.

The artificial ripple bed was made out of wood and was machined on a numerically-controlled milling machine to the following profile.

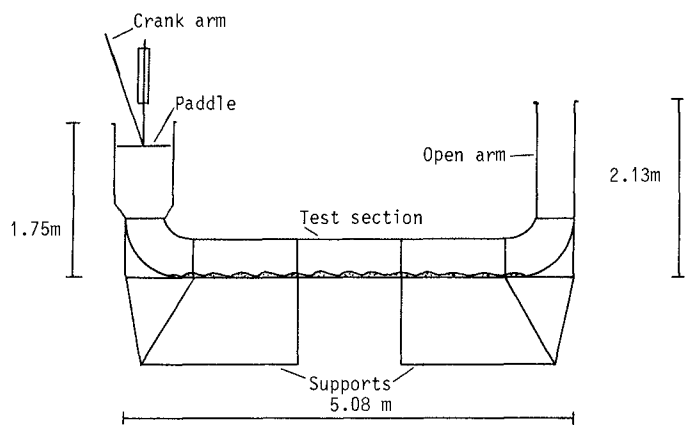

FIG. 2 Sketch of oscillatory flow U-tube

Test	a (m)	T (s)	$\frac{a}{L}$	$\frac{h}{L}$	β/k	$\frac{U_o L}{\nu}$
		(i) Artificial ripples				
32	0.06	3.29	0.6	0.17	15.02	10690.3
33	0.08	3.25	0.8	0.17	15.22	14637.0
34	0.10	3.36	1.0	0.17	15.05	17872.9
35	0.12	3.32	1.2	0.17	15.25	22039.2
36	0.04	3.47	0.4	0.17	14.94	7049.8
37	0.02	3.47	0.2	0.17	14.95	3528.1
38	0.02	1.86	0.2	0.17	19.92	6268.3
39	0.04	1.87	0.4	0.17	19.98	12603.5
40	0.06	1.90	0.6	0.17	19.98	18738.0
41	0.08	1.90	0.8	0.17	19.91	25036.1
42	0.10	1.89	1.0	0.17	20.03	31668.2
43	0.12	1.96	1.2	0.17	19.74	36937.0
44	0.02	5.45	0.2	0.17	12.05	2291.7
45	0.04	5.46	0.4	0.17	12.06	4593.0
46	0.06	5.47	0.6	0.17	11.99	6810.8
47	0.08	5.61	0.8	0.17	11.86	8888.8
48	0.10	5.66	1.0	0.17	11.86	11097.9
49	0.12	5.56	1.2	0.17	12.00	13644.6
		(ii) Self-formed ripples				
11	0.060	3.97	0.79	0.13	10.04	6280.7
84	0.065	3.91	0.72	0.18	12.08	8273.9
87	0.085	4.73	0.71	0.18	14.99	12570.8
90	0.110	4.98	0.67	0.17	19.89	20957.5
96	0.122	5.37	0.71	0.17	19.67	21617.5
97	0.096	4.22	0.83	0.19	15.05	14898.2
98	0.101	3.21	0.74	0.20	20.26	23884.0
99	0.195	4.87	0.77	0.17	30.27	55812.8
100	0.141	3.18	0.67	0.16	31.05	50935.9
101	0.081	5.75	0.75	0.19	12.10	8611.9
102	0.085	4.62	0.86	0.19	12.18	10001.4
103	0.166	4.65	0.68	0.18	30.54	49852.9
104	0.108	3.80	0.72	0.20	19.97	22676.9

TABLE 1. Test conditions

$$y = \tfrac{1}{2}h(\cos k\xi - 1), \quad x = \xi - \tfrac{1}{2}h \sin k\xi \qquad (1)$$

where the crest-to-trough height h of the ripple was 0.017 m and the wavelength $2\pi/k$ was 0.10 m. This profile was very similar to that of the ripples which form with the 0.41 mm sand.

Further details of the experimental equipment are given by Du Toit (1980).

3. TEST PROCEDURE AND RESULTS

At least one day prior to a test the tank was filled with tap water and left to de-aerate. Natural sand ripples were obtained by selecting the appropriate frequency and amplitude of oscillation and letting the rig run until the ripples reached their equilibrium profile. The rig was then stopped and the ripple geometry measured. On the day of the test the equipment was left on for at least an hour to warm up.

At least two vertical traverses were made during each test. For each traverse records of at least thirty cycles were made at various fixed heights above the bed. In all the tests traverses were made above a ripple crest and a ripple trough when the tray was in its central position. In some tests in the oscillatory flow U-tube two additional traverses were made a sixth and a third of a ripple length from the crest.

The water temperature and output from the various instruments were checked regularly during and the ripple geometry at the end of a test to ensure that no significant changes had taken place.

The conditions under which the various tests were carried out are summarized in Table 1. All the tests were in the fully-developed rough turbulent regime according to the criteria of Kajiura (1968), Sleath (1974a), Kamphuis (1975) and Jonsson (1980), except for a few tests with artificial ripples at the shorter amplitudes of oscillation.

3.1 Ripple and velocity similarity

It has been claimed, e.g. Brebner & Collins (1961), that flow fields simulated in the oscillating tray rig and the oscillatory flow U-tube are not dynamically similar. However, if the ripples are similar, Sleath (1974b) showed theoretically that the flow fields are dynamically similar.

A plot of ripple lengths against the corresponding amplitudes of oscillation for which the ripples had been obtained, is shown in Figure 3.

Added to the present data, are the experimental results of a large number of undergraduates, cf. Sleath & Ellis (1979), at the University of Cambridge in the same oscillating tray rig with the same 0.41 mm sand as the present study.

These are compared with the empirical predictions of Mogridge & Kamphuis (1972) and Sleath (1975), obtained from experiments conducted in wave flumes and oscillatory flow U-tubes.

The minimum and maximum Reynolds numbers $U_0/\sqrt{\omega\nu}$ obtained in the present experiments were respectively 42 and 207. The predictions of Sleath for these two values are shown in the figure.

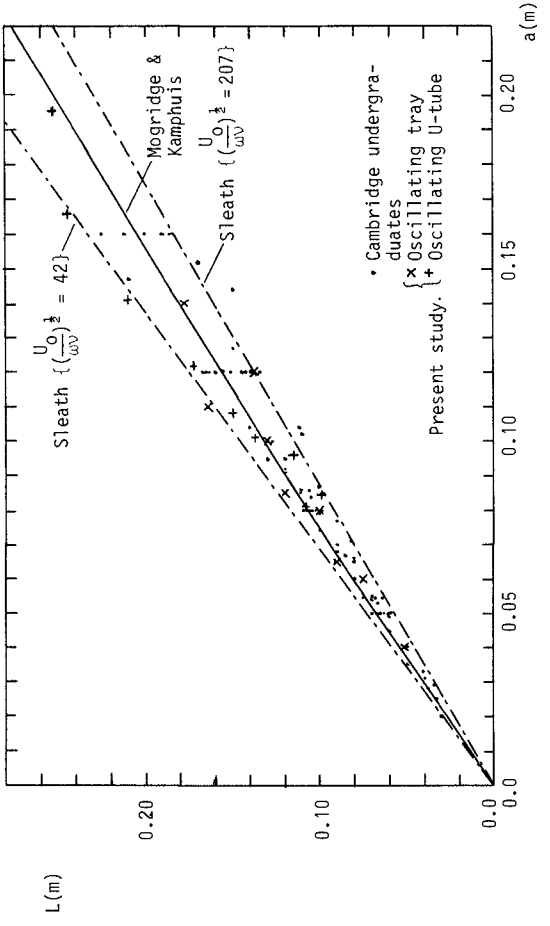

FIG. 3 Variation of ripple length with amplitude of motion

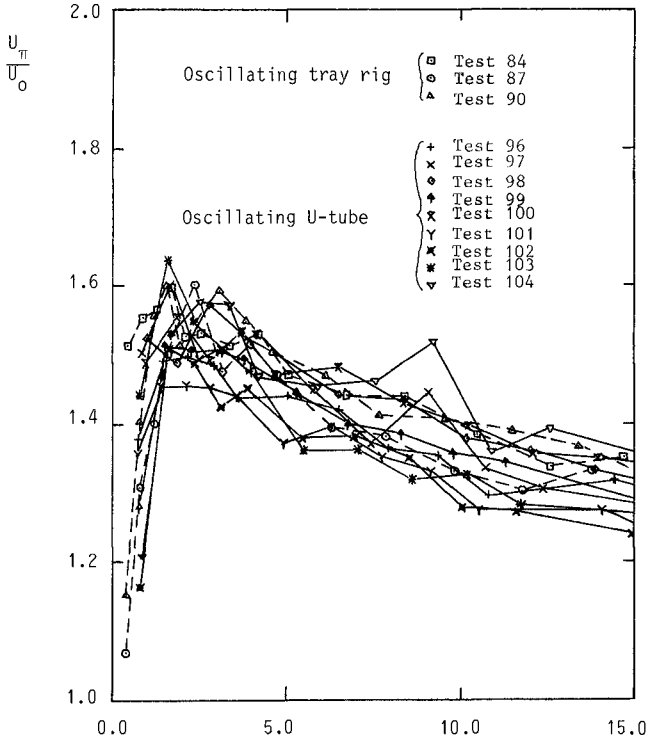

FIG. 4 Variation of $\frac{U_\pi}{U_o}$ with βy above ripple crest

The agreement between the various experiments and the predictions is quite close and there doesn't seem to be any consistent difference between the results obtained in the two different rigs. The ripple lengths obtained in the two cases are, therefore, similar.

In the case of the oscillating tray rig, the ripple is oscillating forwards and backwards past the measuring volume. The only instants, therefore, during the cycle when the velocities can be compared with those measured in the oscillatory flow U-tube for $\frac{a}{L} < 1.0$ and a vertical traverse above the crest, are when the measuring volume is directly above a crest. This occurs at $\omega t = 0$ and $\omega t = \pi$ and corresponds to maximum tray velocity for the

oscillating tray rig and maximum free stream velocity for the oscillatory flow U-tube.

Figure 4 shows how the non-dimensional velocities U_π/U_o change with distance βy above the ripple crest, where

$$\frac{U_\pi}{U_o} = \frac{1}{2U_o} \{U(\omega t = o) - U(\omega t = \pi)\} \quad (2)$$

and $\beta = \sqrt{\frac{\omega}{2\nu}}$. The oscillating flow U-tube velocities were converted to oscillating tray velocities by

$$\frac{U_\pi \text{ (tray)}}{U_o} = 1 - \frac{U_\pi \text{(U-tube)}}{U_o} \quad (3)$$

considering the variation in $\frac{\beta}{k}$, $\frac{h}{L}$ and $\frac{a}{L}$ for the various tests, the agreement is good and there seems to be not apparent difference between the velocity profiles obtained in the oscillating tray rig and the oscillatory flow U-tube. The velocities can, therefore, be taken as similar.

Due to the similarity in ripple lengths and velocity profiles it can, therefore, be concluded that the flow fields simulated in the two rigs are dynamically similar.

3.2 Velocities above an oscillating fixed ripple

The way in which $\frac{U}{U_o}$ changes with ωt for various positions above an oscillating fixed ripple is shown in Figure 5. Figures 5 (a) and (b) are for a crest traverse and Figures 5 (c) and (d) for a trough traverse. The instants when the measuring volume was directly above a crest are indicated in the figure with crosses. It should also be noted that the tray was travelling with the velocity $-U_o \cos \omega t$.

When a rippled bed is oscillated, the fluid in the viscous part of the boundary layer has to travel along with the ripple surface. However, in the outer layer the fluid moves over the crest in a direction opposite to that of the ripple surface, continuity then requires that the fluid over the trough should move in the same direction as the ripple surface. These features are clearly illustrated in Figure 5.

In Figure 5 (a) it can be seen that there is a sharp increase in the velocity in the direction opposite to that in which the ripple is travelling as the crest approaches the measuring volume. This corresponds to the fluid in the outer layer spilling over the ripple crest. As the viscous layer moves past the measuring volume there is a sudden switch in

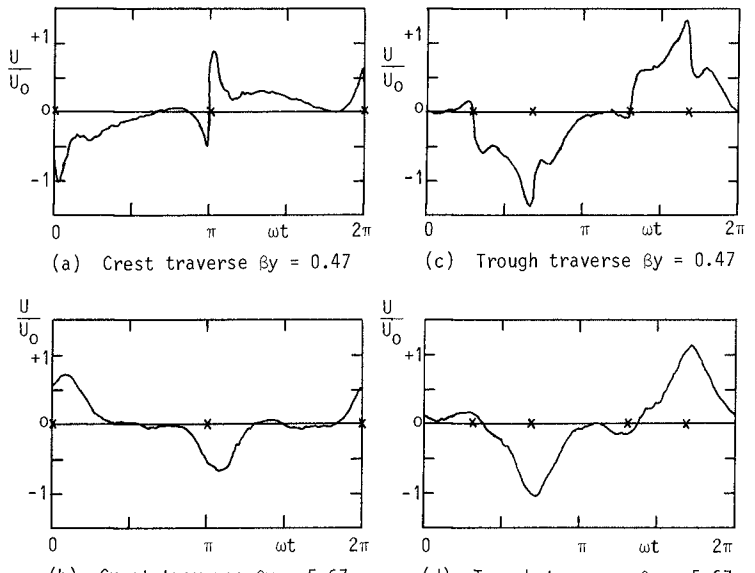

FIG. 5 TEST 32: Average velocity cycles for βy = 0.47 and 5.67 for crest and trough traverses

the velocity direction due to the viscous layer travelling with the ripple. This can be observed in Figure 5 (c) as well, though very much weaker. This viscous effect diminishes quickly and in Figure 5 (b) & 5 (d) it can not be observed any more. There the measuring volume is in the outer layer all the time.

An additional phenomenon can be observed in Figures 5 (c) & 5 (d). Very prominent peaks occur in the velocity cycles at $\omega t = 0.65\pi$ and 1.65π. These peaks occur just after flow reversal and correspond to the fluid surging over the ripple in the direction opposite to that in which the ripple is travelling. It is also associated with the ejection of the vortex which has been on the downstream side of ripple prior to flow reversal. This effect can be seen in the photographs published by Bagnold (1946).

3.3 Velocities above a stationary sand ripple

In contrast with the previous Figure, Figure 6 (a) shows the average velocity for βy = 1.44 above a ripple crest and Figure 6 (b) shows the average velocity cycle for βy = 1.18 above a ripple trough for stationary sand ripple in the

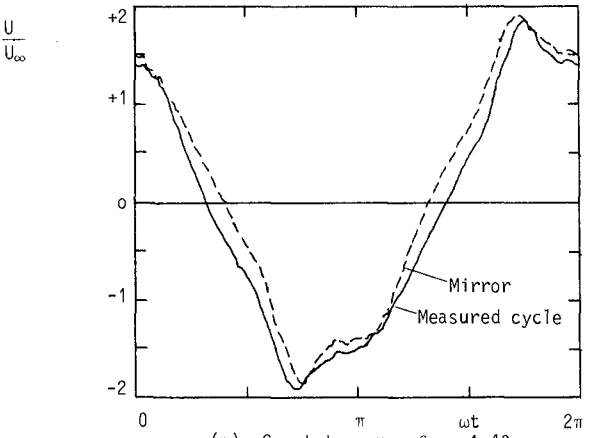

(a) Crest traverse $\beta y = 1.40$

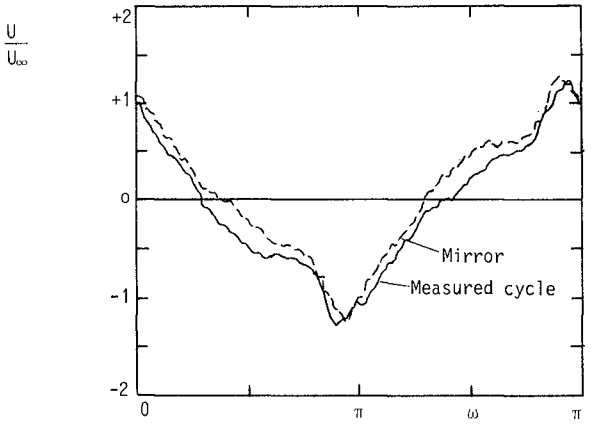

(b) Trough traverse $\beta y = 1.47$

FIG. 6 TEST 101: Average velocity cycles for $\beta y \approx 1.4$ for crest and trough traverses.

oscillatory flow U-tube. Also shown on the Figures are the "mirror" plots of the measured average velocity cycles. These were obtained by shifting the average velocity cycles by π radians and inverting them. Thus the difference between the two curves provides an indication of the magnitude of

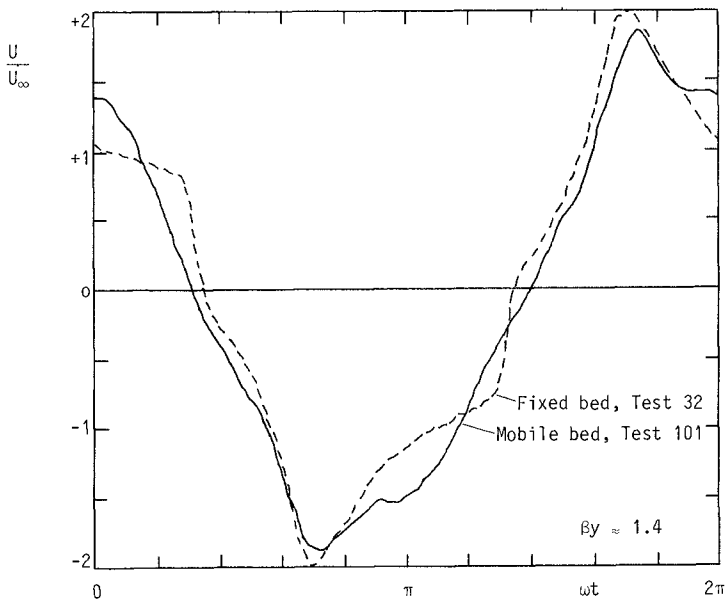

FIG. 7 Comparison between fixed bed and mobile bed velocity cycles.

experimental errors such as mean drift in the tank.

A prominent feature in both figures is the occurence of a peak in the velocity cycle at $\omega t = 0.9\pi$ and 1.9π for the trough plot. During the course of the experiments it was observed that the crest swayed from side to side, forming a small cusp of sand first on one side and then, as the flow reversed, on the other side. It was originally thought that the presence of the peak in the velocity cycles was due the swaying of the crest. However, comparison with results obtained for the fixed wooden bed in the oscillatory tray rig showed the same peak. This is illustrated in Figure 7, where the oscillatory tray velocities were converted to oscillating free stream results.

This peak corresponds to the strong surge of fluid going over the ripple crest and sweeping through the ripple trough, as illustrated in the photographs by Bagnold (1946). The surge occurs just after flow reversal and is associated with the ejection of the vortex which had been on the downstream side of the ripple prior to flow reversal.

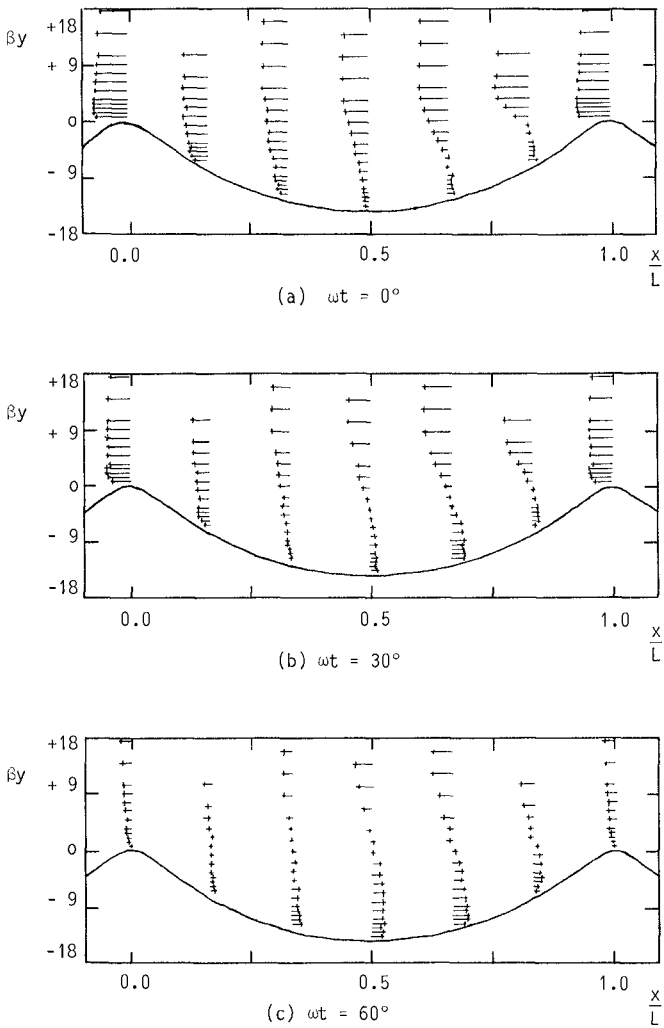

FIG. 8 Variation of the horizontal velocity component of the flow field above a rippled bed with time.

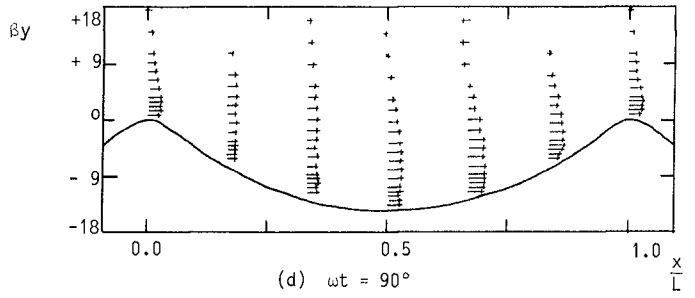

(d) ωt = 90°

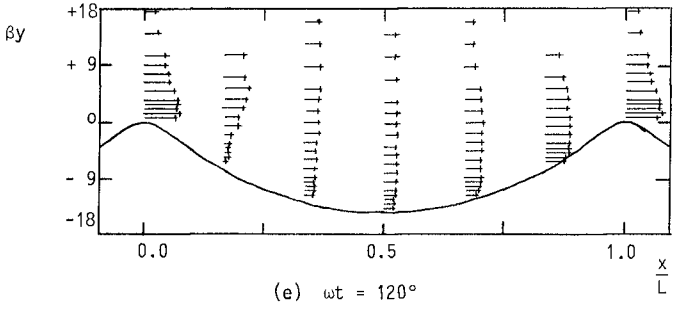

(e) ωt = 120°

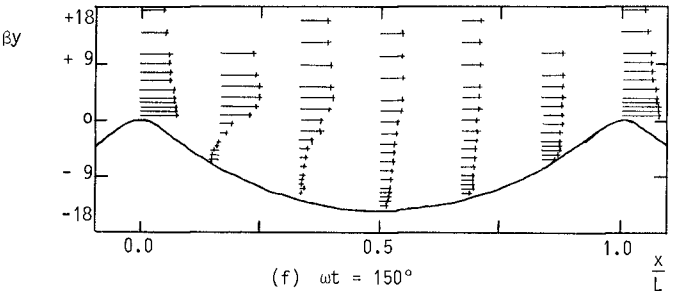

(f) ωt = 150°

FIG. 8 Variation of the horizontal velocity component of the flow field above a rippled bed with time.

Thus although the change in position of the crest cusp is not the cause of the velocity peak, the velocity peak may be the cause of change in position.

The variation in the horizontal velocities in the flow field above a rippled bed during a half cycle is illustrated in Figure 8.

Only the instants $\omega t = 0$, $\pi/6$, $\pi/3$, $\pi/2$, $2\pi/3$ and $5\pi/6$ are shown.

In Figure 8 (a) the freestream is moving with maximum velocity from right to left and a well defined vortex fills almost half the ripple trough on the downstream side of the ripple. As the freestream decelerates, the vortex increases in size, Figure 8 (b), until it fills almost the whole trough, Figure 8 (c). Although the freestream has not reversed yet at this instant, $\omega t = 2\pi/3$, the flow near the ripple crest is on the brink of reversing. In Figure 8 (d) the freestream reverses. The vortex is being ejected over the crest and a strong surge of fluid sweeping through the ripple trough and spilling over the crest is building up. At $\omega t = 2\pi/3$, Figure 8 (e), the flow has already started separating at the crest and a new vortex starts to form. A jet, associated with the separation, shoots out over the trough and at $\omega t = 5\pi/6$ it has almost reached the trough.

The general flow features show good agreement with those photographed by Bagnold (1946), despite the differences in flow conditions and ripple geometry. Sawamoto et al (1980) used a ripple profile with a smaller steepness and a much more rounded crest and, therefore, the vortex was not as pronounced as in the present study.

4. CONCLUSIONS

The range of flow conditions covered during the present series of tests covers a wide spectrum of conditions encountered in practice. It is believed that the present results could help to improve our understanding of the boundary layer in oscillatory flow over rippled beds and lead to a better understanding of the associated phenomena.

The author would like to thank Dr. J F A Sleath of the University of Cambridge for his encouragement, as well as the South African CSIR, the British NERC and the Sir Henry Strakosch Memorial Trust for their financial support.

5. REFERENCES

BAGNOLD, R A (1946). Motion of waves in shallow water. Interaction of waves and sand bottoms. Proc. Roy. Soc., A 187, pp. 1-15.

BREBNER, A & COLLINS, J I (1961). The effect on mass transport of the onset of turbulence at the bed under periodic gravity waves. ASME Hydraulics Conf., Paper No. 61-EIC-8.

DU TOIT, C G (1980). Velocities close to a bed of sand in oscillatory flow. Ph.D. thesis, University of Cambridge.

DU TOIT, C G & SLEATH, J F A (1981). Velocity measurements close to rippled beds in oscillatory flow. J. Fluid Mech., 112, pp. 71-96.

HORIKAWA, K & WATANABE, A (1970). Turbulence and sediment concentration due to waves. Proc. 12th Conf. Coastal Engng., pp. 751-765.

JONSSON, I G (1980). A new approach to oscillatory rough turbulent boundary layer flow. Ocean Engng.,7, pp. 109-152.

KAJIURA, K (1968). A model of the bottom boundary in water waves. Bull. Earthquake Res. Inst., 46, pp. 75-123.

KAMPHUIS, J W (1975). Friction factor under oscillatory waves. J Waterways, Harbors & Coastal Engng. Div., 101 (WW2), pp. 135-144.

MOGRIDGE, G R & KAMPHUIS, J W (1972). Experiments on bed form generation by wave action. Proc. 13th Conf. Coastal Engng., pp. 1123-1142.

NAKATO, T, LOCHER, F A, GLOVER, J R & KENNEDY, J F (1977). Wave entrainment of sediment from rippled beds. J Waterways, Ports, Coastal & Ocean Div., 103 (WW1), pp. 83-99.

SAWAMOTO, M YAMASHITA, T & KURITA, T (1980). Vortex formation over rippled bed under oscillatory flow. Tech. Rep. No. 27, Dept. Civ. Engng. Tokyo Inst. Tech., pp. 75-85.

SLEATH, J F A (1974a). Stability of laminar flow at seabed. J Waterways, Harbors & Coastal Engng. Div., 100 (WW2), pp.105-123.

SLEATH, J F A (1974b). Velocities above a rough bed in oscillatory flow. J Waterways, Harbors & Coastal Div., 100 (WW4), pp. 287-304.

SLEATH, J F A (1975). A contribution to the study of vortex ripples. J Hyd. Res., 13 (3), pp. 315-328.

SLEATH, J F A & ELLIS, A C (1979). Ripple geometry in oscillatory flow. CUED/A - Hydraulics/TR2.

6. SYMBOLS

a = Amplitude of oscillation

h = ripple height

k = ripple frequency

= $2\pi/L$

L = ripple length

T = period of oscillation

t = time

U_o = maximum oscillating tray velocity

U_∞ = maximum freestream velocity

U_π = velocity at $\omega t = \pi$

β = measure of laminar boundary layer thickness

= $(\frac{\omega}{2\nu})^{\frac{1}{2}}$

ω = oscillation frequency

= $2\pi/T$

ν = kinematic viscosity of fluid